# Final Report: Use of Advanced Composites for Hawaii Bridges

H. Ronald Riggs

Si-Hwan Park

Ian N. Robertson

Gregor Fischer

Prepared in Cooperation with:

State of Hawaii, Department of Transportation, Highways Division

and

U.S. Department of Transportation, Federal Highway Administration

UNIVERSITY OF HAWAII
COLLEGE OF ENGINEERING

DEPARTMENT OF CIVIL AND ENVIRONMENTAL ENGINEERING

Research Report UHM/CEE/04-07
December 2004

**Technical Report Documentation Page**

| 1. Report No. HWY-L-2001-01 | 2. Government Accession No | 3. Recipient's Catalog No |
|---|---|---|
| 4. Title and Subtitle: Final Report: Use of Advanced Composites for Hawaii Bridges | | 5. Report Date: December 28, 2004 |
| | | 6. Performing Organization Code |
| 7. Authors: H.R. Riggs, S.H. Park, I.N. Robertson, G. Fischer | | 8. Performing Organization Report No. |
| 9. Performing Organization Name and Address: Department of Civil and Environmental Engineering, University of Hawaii at Manoa, 2540 Dole St. Holmes Hall 383, Honolulu, HI 96822 | | 10. Work Unit No. (TRAIS) |
| | | 11. Contract or Grant No. 47770 |
| 12. Sponsoring Agency Name and Address: Hawaii Department of Transportation, Highways Division, 869 Punchbowl St., Honolulu, HI 96813 | | 13. Type of Report and Period Covered: Final – Phase 2 – Volume 1, 5/01 – 4/04 |
| | | 14. Sponsoring Agency Code |

15. Supplementary Notes

Prepared in cooperation with the U.S. Department of Transportation, Federal Highway Administration

16. Abstract

The research project 'Use of Advanced Composites for Hawaii Bridges with Application to Renovation of Historic Bridges' was funded by the Hawaii Department of Transportation and carried out at the University of Hawaii at Manoa. This is volume 1 of the project's final report. The primary purpose of this volume is to summarize the information contained in previous reports and documents and to provide some information not previously reported.

There were several, distinct phases to the project. In phase 1, the report, 'A Primer for FRP Strengthening of Structurally Deficient Bridges' was published. This report is a useful introduction and overview of the topic and is appropriate as a first resource for engineers entering the topic. It is briefly summarized herein.

Another phase of the project involved the groundwork to use FRP on one of Hawaii's deficient bridges. A candidate bridge was identified and a proposal was submitted to the FHWA Innovative Bridge Research and Construction (IBRC) program. The proposal was funded, and that project is on-going. That project can be viewed as a follow-on of this project. The bridge is a prestressed concrete girder bridge that is experiencing shear cracking. Evaluation revealed that it is deficient in shear. Part of this project involved providing technical assistance regarding the possible use of FRP to strengthen the bridge. The IBRC project itself involves instrumenting and monitoring the retrofit to evaluate the FRP performance. The technical content of the proposal is contained herein, as it is not readily available elsewhere. The proposal clearly identifies the work that is to be carried out in the IBRC project.

Another task in the current project was to carry out experimental testing of FRP shear retrofit on a prestressed concrete girder. This work is reported in volume 2 of this final report.

The issue of bond between FRP and concrete is a critical one for the success of 'bond-critical' retrofits. The bond mechanism is quite complex and is not completely understood. To gain a better understanding of the phenomenon for future applications, experimental and computational efforts were initiated in this project and are being continued in the IBRC project. The results of literature surveys on experimental testing of bond between FRP and concrete and on the computational modeling of fracture and debonding in concrete are presented here.

| 17. Key Words | 18. Distribution Statement |
|---|---|
| Fiber reinforced polymer (FRP)<br>Structurally deficient bridges | No restriction. This document is available to the public through the National Technical Information Service 5285 Port Royal Road, Springfield VA 22161 |

| 19. Security Classif.(of this report) | 20. Security Classif. (of this page) | 21. No. of Pages | 22. Price |
|---|---|---|---|
| Unclassified | Unclassified | 39 | |

**Form DOT F 1700.7** (8-72) Reproduction of completed page authorized

# Executive Summary

The research project 'Use of Advanced Composites for Hawaii Bridges with Application to Renovation of Historic Bridges' was funded by the Hawaii Department of Transportation and carried out at the University of Hawaii at Manoa. This is volume 1 of the project's final report. The primary purpose of this volume is to summarize the information contained in previous reports and documents and to provide some information not previously reported.

There were several, distinct phases to the project. In phase 1, the report, 'A Primer for FRP Strengthening of Structurally Deficient Bridges' was published. This report is a useful introduction and overview of the topic and is appropriate as a first resource for engineers entering the topic. It is briefly summarized herein, and the full report is available on-line.

Another phase of the project involved the groundwork to use FRP on one of Hawaii's deficient bridges. A candidate bridge was identified and a proposal was submitted to the FHWA Innovative Bridge Research and Construction (IBRC) program. The proposal was funded, and that project is on-going. That project can be viewed as a follow-on of this project. The bridge is a prestressed concrete girder bridge that is experiencing shear cracking. Evaluation revealed that it is deficient in shear. Part of this project involved providing technical assistance regarding the possible use of FRP to strengthen the bridge. The IBRC project itself involves instrumenting and monitoring the retrofit to evaluate the FRP performance. The technical content of the proposal is contained herein, as it is not readily available elsewhere. The proposal clearly identifies the work that is to be carried out in the IBRC project.

Another task in the current project was to carry out experimental testing of FRP shear retrofit on a prestressed concrete girder. This work is reported in volume 2 of this final report, and it is available on-line.

The issue of bond between FRP and concrete is a critical one for the success of 'bond-critical' retrofits. The bond mechanism is quite complex and is not completely understood. To gain a better understanding of the phenomenon for future applications, experimental and computational efforts were initiated in this project and are being

continued in the IBRC project. The results of literature surveys on experimental testing of bond between FRP and concrete and on the computational modeling of fracture and debonding in concrete are presented here.

## Acknowledgements

This report was produced under Hawaii Department of Transportation's Project No. HWY-L-2001-01, 'Use of Advanced Composites for Hawaii Bridges with Application to Renovation of Historic Bridges,' with the University of Hawaii at Manoa. Mr. Paul Santo, Bridge Design Section, HDOT, was the technical contact.

The authors gratefully acknowledge the support received under this project.


**Disclaimer**

The contents of this report reflect the views of the authors, who are responsible for the facts and accuracy of the data presented herein. The contents do no necessarily reflect the official views or policies of the State of Hawaii, Department of Transportation or the Federal Highway Administration. This report does not constitute a standard, specification, or regulation.

# Table of Contents

# List of Figures

# 1.0 Introduction

Fiber-reinforced polymers (FRP) have been used widely in the aerospace and automobile industries. As such, engineers and fabricators in those fields are experienced in its application, and the material has a reasonably long track record. However, its use in structural engineering applications, such as bridges and buildings, is relatively new. Engineers and contractors in this area are not as familiar with the material, and they are therefore not as comfortable designing with this material as with the familiar materials of concrete, steel, and wood. In addition, the material itself does not have as long a track record in these applications. Nevertheless, the advantages of FRP for specific applications result in it being used more and more frequently for structural engineering applications. To date, many of the uses have been in strengthening and retrofitting existing structures made of reinforced concrete or masonry. Some application of FRP has also been made to new construction where it is the primary structural material.

One area in which FRP is being used more and more is the strengthening of structurally deficient concrete bridges. As is widely known, a significant percentage of the bridges in the U.S. are deficient, and FRP is being used together with traditional materials and approaches for the repair and upgrading of these bridges. A major goal in many applications has been to increase the load rating of older bridges without adversely affecting bridge aesthetics.

Incentives for the use of FRP over traditional materials include the material's high stiffness-to-weight and strength-to-weight ratios, corrosion resistance, and constructability. Disincentives include unfamiliarity by engineers, cost, proprietary nature of the material, and lack of experienced construction personnel.

In this context, the Department of Civil and Environmental Engineering at the University of Hawaii at Manoa has carried out a research project titled 'Use of Advanced Composites for Hawaii Bridges with Application to Renovation of Historic Bridges', funded by the Hawaii Department of Transportation. This is volume 1 of the project's final report. The project had 3 main components: 1) development of an introduction to the use of FRP to retrofit structurally deficient bridges; 2) experimental testing of FRP shear retrofit of prestressed concrete girders; and 3) identification and planning for an

IBRC FRP retrofit project. The report ‘A Primer for FRP Strengthening of Structurally Deficient Bridges’ was published in 2002. Volume 2 of the final report contains detailed results of a major experimental program. The purpose of this volume is primarily to summarize the other reports and to put them into context of the overall project. It also provides results of additional new work which is being continued under the IBRC project.

Chapter 2 reproduces the executive summary of the report ‘A Primer for FRP Strengthening of Structurally Deficient Bridges’, together with information on how to obtain a copy. Chapter 3 reproduces the technical content of the IBRC proposal, because it is not widely available elsewhere. The proposed project was funded, and work commenced in November 2003. For the IBRC project, and all future applications, a better understanding of the bond between FRP and concrete is desireable. This is a focus of the IBRC project, and some initial work was carried out under the current project. Work reported on herein includes literature surveys of experimental and computational work related to bond between FRP and concrete. These appear in Chapters 4 and 5.

# 2.0 A Primer for FRP Strengthening of Structurally Deficient Bridges

## 2.1 Overview

The following is the executive summary from the report ‘A Primer for FRP Strengthening of Structurally Deficient Bridges’. The full report is available for free download on-line at <http://cee.hawaii.edu/reports/UHM-CEE-02-03.pdf>.

## 2.2 Summary

Although fiber-reinforced polymers (FRP) have been used widely in the aerospace and automobile industries, its use in bridges and buildings is relatively new. Engineers and contractors in this area are not as comfortable designing with FRP as with the familiar materials of concrete, steel, and wood. In addition, the material itself does not have as long a track record in these applications. Nevertheless, the advantages of FRP for specific applications result in it being used more and more frequently for structural engineering applications, especially for strengthening and retrofitting existing structures made of reinforced concrete or masonry.

One area in which FRP is being used more frequently is the strengthening of structurally deficient concrete bridges. Incentives for the use of FRP over traditional materials include the material’s high stiffness-to-weight and strength-to-weight ratios, corrosion resistance, and constructability. Disincentives include unfamiliarity by engineers, cost, proprietary nature of the material, and lack of experienced construction personnel.

The objective of this report is to provide the Hawaii Department of Transportation with a ‘primer’ for the use of FRP in strengthening structurally deficient concrete bridges. Its aim is to increase the engineer’s familiarity with the products, and thereby contribute to the consideration of FRP for specific projects based on technical merit. It represents a first reference that engineers can use for a concise description of FRP, recent relevant applications, overview of the materials, and basic how-to design procedures and guidelines, including possible design solutions for common situations. Because FRP is a relatively new material with a relatively short track record in the area of bridge strengthening, field instrumentation, testing, and monitoring of the immediate and long-term behavior of FRP strengthened bridges are also discussed.

This report draws heavily on other published reports and papers. It is not meant as a complete reference, but rather it directs the reader to more comprehensive documents for specific issues.

# 3.0 IBRC Proposal

## 3.1 Overview

A proposal to instrument the FRP shear retrofit of the Salt Lake Boulevard Bridge over Halawa Stream in Honolulu was submitted to the FHWA's Innovative Bridge Research and Construction (IBRC) program. The proposed work involves the instrumenting and long-term monitoring of the FRP to evaluate its performance, especially to identify if debonding occurs with the cyclic live loading that bridges experience. The project was funded, and work commenced in November 2003. The technical content of the proposal is reproduced herein so that the scope of that project, which can be viewed as a follow-on to this project, can be clearly understood.

## 3.2 Summary

The Salt Lake Boulevard Bridge over Halawa Stream is a 3-span, continuous, prestressed concrete girder bridge. The 150-ft long, 100-ft wide bridge carries six lanes of heavy traffic. It has been determined that the shear capacity of some girders is inadequate. Furthermore, visual inspection has revealed that 16 girders have hairline diagonal shear cracks near the supports. These shear cracks are potentially quite serious. As a result, the City and County of Honolulu plans to strengthen the girders in shear. Although a specific strengthening system has not yet been selected, an FRP composite system appears to be the best alternative. It is anticipated that a strengthening system will be selected in the first half of 2003.

If an FRP system is chosen, the principal investigators propose herein to instrument the FRP to measure its effectiveness under the dynamic traffic loads. Of particular interest is the possible delamination over extended periods caused by the dynamic loading and the resulting strain concentration as a result of movement of the existing cracks. We intend to monitor the performance of the FRP over several years. Should delamination occur, proper anchoring of the FRP, especially around reentrant corners and at the top and bottom, will be critical to its effectiveness.

We propose to embed high fidelity, fiber optic sensors in the FRP layers as they are applied to the bridge. The shear strains in the girders will be quite small, and electrical resistance strain gages are inadequate to measure the strain with sufficient accuracy. High fidelity, fiber optic sensors, on the other hand, can measure very small strains. Sensors will be located both on the crack and above and below the crack. Measuring strains throughout the depth of the girders will allow delamination to be detected. A remote data acquisition system will be used so that the strain data will be transmitted continuously to our laboratory. Some data will be processed in real time and made available on a web site, so that authorized users, such as the city and state transportation departments, can observe the tests in real time.

Finite element analysis of both uncracked and cracked, reinforced sections will be carried out to determine the theoretical shear strain distribution in the AASHTO-shaped girders. These predictions help in the placement of the strain gages. They will also be compared to the measured data.

### 3.3 Introduction

The Salt Lake Boulevard Bridge over Halawa Stream is a 3-span, continuous, prestressed concrete girder bridge that is supported on concrete piles and pier caps. The bridge was built in 1968, and it was subsequently widened around 1988. Figure 1 shows the bridge elevation, while Figure 2 shows more clearly the girders from underneath. The bridge is 150 ft long and 100 ft wide, and it carries six lanes of traffic plus a median. Salt Lake Blvd. is a major thoroughfare and it carries heavy traffic. The bridge belongs to the City and County of Honolulu.

As a result of a bridge inspection and evaluation program, it was determined from the load rating calculations that the shear capacity of some girders is inadequate (Shigemura 2001). The operating RF for the original girders is as low as 0.87, while the corresponding inventory RF is 0.52. Subsequent visual inspection revealed that 16 of the girders have hairline diagonal shear cracks near the supports. All 16 girders are in the original section of the bridge. The locations of the cracks are shown in Figure 3, where the cracked sections are shaded black (Shigemura 2001). Photographs of two of the cracked girders are shown in Figure 4.

The shear cracks are potentially quite serious. As a result, the City and County of Honolulu plans to strengthen the girders in shear. The design work is scheduled to begin in early 2003, and construction is planned for the spring of 2004. The design consultant will recommend a strengthening system, and therefore a system has not yet been selected. However, at this point an FRP system appears to be the best alternative.

If an FRP system is chosen, the principal investigators propose herein to instrument the FRP to measure its effectiveness under the dynamic traffic loads. Of particular interest is the possible delamination over extended periods caused by the dynamic loading and the resulting strain concentration as a result of movement of the existing cracks. Some FRP manufacturers have called attention to possible delamination and crushing of fibers over existing cracks. This issue is discussed in ACI 440R-02 (ACI 2002), section 5.4.1.2. It is recommended therein that larger cracks (> 0.010 in. or 0.3 mm) should be pressure injected with epoxy prior to the application of the FRP. However, this is not possible with the hairline shear cracks. In addition, it is unknown whether or not long-term dynamic loading will cause delamination as a result of preexisting smaller cracks. Therefore, we intend to monitor the performance of the FRP over several years.

From the data collected it will be possible to determine both the existence and the extent (if any) of the delamination. The sensors will not interfere with the integrity of the FRP. If the FRP does experience delamination as a result of dynamic loading on the bridge, the anchoring of the FRP strips will be critical to the integrity of the strengthening system. The anchoring should be considered carefully (Park et al. 2002) because of the shape of the girder cross section; see Figure 5. The FRP must be prevented from peeling away from the two reentrant corners on each side of the girder.

**Figure 1 Salt Lake Blvd. Bridge**


**Figure 2 Underside of bridge**

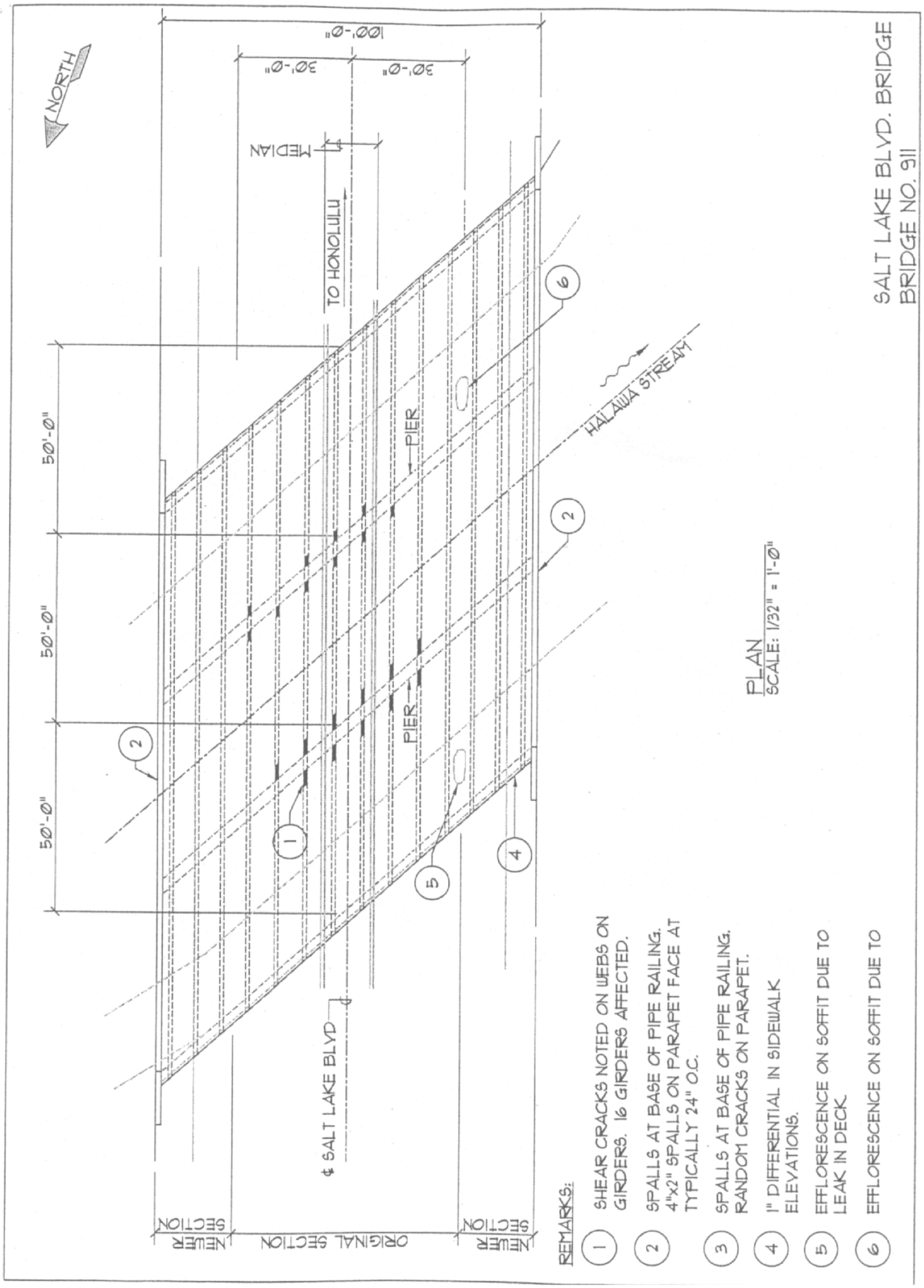


**Figure 3 Cracked girder locations (Shigemura 2001)**

**Figure 4 Girders with shear cracks (Shigemura 2001)**

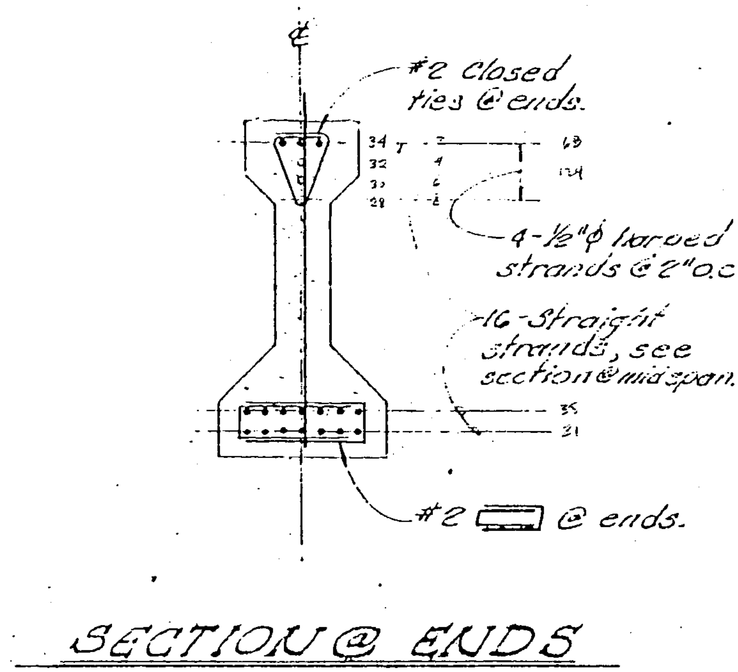


**Figure 5 Girder cross section (Shigemura 2001)**

## 3.4 Project Overview

As explained in the previous section, the Salt Lake Boulevard Bridge over Halawa Stream (hereinafter referred to as the bridge) has numerous girders deficient in shear capacity; some of these girders have visually detectable shear cracks. As a result, the City and County of Honolulu will strengthen the bridge in shear. If an FRP system is chosen, a wet lay-up will almost certainly be used, possibly with multiple layers. We propose to instrument and monitor the performance of the FRP strengthening system. To achieve this, we propose to embed high fidelity, fiber optic strain gages in the FRP layers as they are applied to the bridge. The shear strains in the girders will be quite small, and electrical resistance strain gages are inadequate to measure the strain with sufficient accuracy. High fidelity, fiber optic sensors, on the other hand, can measure very small strains and do not suffer the drift typical of the electrical resistance gages. Sensors will be located both on the crack and above and below the crack. Measuring strains throughout the depth of the girder will allow delamination to be detected. A remote data acquisition system will be used so that the strain data will be transmitted continuously to our laboratory. Some data will be processed in real time and made available on a web site so that authorized users, such as the city and state transportation departments, can observe the tests in real time.

After retrofitting of the bridge is complete, load tests with trucks of known weight will be carried out. These load tests, with heavier loads than the bridge will see under normal traffic, will allow us to validate the initial effectiveness of the FRP and the accuracy of the instrumentation. These measured results will be compared to analytical predictions.

Analytical work prior to the retrofit will be carried out to 1) optimize the design and placement of the instrumentation system, and 2) provide benchmark data against which the load test results can be evaluated. We anticipate that approximately 5 girders will be instrumented. The analyses will be used to identify the heaviest loaded girders. In addition, a more detailed visual examination will be made to identify the most severely cracked girders. The instrumented girders will be chosen based on the analytical model and the visual inspection. In addition, we intend to instrument approximately 2 uncracked girders as controls.

The bridge will continue to be monitored over 3 years. This will reveal if any delamination occurs over time with the usual dynamic loading of the bridge.

The next sections discuss in more detail the instrumentation, monitoring, load tests, and analytical work.

### 3.5 Instrumentation

To monitor the FRP shear reinforcement for potential delamination from the beam webs, it is proposed that fiber optic strain sensors be located in the FRP at various locations relative to the existing cracks. By monitoring the strain in the FRP at the crack and at prescribed distances from the crack, it will be possible to determine if and when the FRP starts to delaminate from the concrete surface. Fatigue testing of concrete bridge girders with externally bonded FRP reinforcement has shown a potential for delamination (Aidoo 2002).

At the ultimate load condition, the large deformations anticipated at flexural and shear cracks will cause large-scale delamination of externally bonded FRP. It is therefore important that adequate anchorage be provided at either end of the FRP, and at reentrant corners, so that the reinforcement remains effective at the ultimate limit state, regardless of the extent of delamination. However, at the serviceability load level, it is desirable that the FRP remain fully bonded to the concrete surface so as to avoid compression buckling or fatigue failure as a result of service load induced movement across the existing shear cracks. The instrumentation and monitoring program outlined here will provide warning of the initiation of delamination so that corrective measures can be taken before further damage occurs.

### 3.5.1 Fiber Optic Strain Sensors

Under service load conditions, the strains in the FRP shear reinforcement will be on the order of 10 to 20 microstrain. To measure these strains accurately and reliably in field conditions, it is proposed that fiber optic strain sensors be embedded in the FRP fabric during installation. Fiber optic strain sensors are extremely small (Figure 6) and can easily be embedded between two layers of FRP fabric without jeopardizing the performance of the FRP.

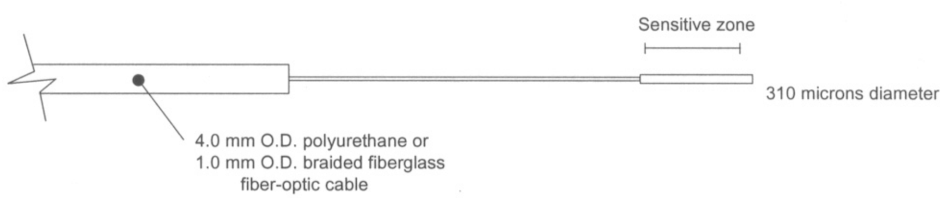


**Figure 6 Typical fiber optic strain gage**

These gages have been shown to provide excellent accuracy and long-term stability both in laboratory and field conditions (McKinley 2002) and are well suited to the proposed application. They are immune to electro-magnetic interference and do not deteriorate from corrosion or exposure to moisture as may occur with externally applied electrical resistance gages.

Two types of fiber optic sensor will be considered for this application. Fabry Perot or Gap-type sensors use a light source to measure accurately the distance between the end of an optical fiber and a reflective surface, as shown in Figure 7. Bragg Grating sensors monitor the frequency of light reflected by a refractive index 'grating' impressed on the fiber core. As the fiber is deformed axially, the spacing of the grating changes and a different frequency light is reflected (Figure 8). Both types of sensor are commercially available with rugged lead wires and optical connectors to withstand the rigors of field installation. The sensors will be monitored by a data acquisition system installed at the site, and the data will be relayed via telemetry to UH for real-time processing. Graphical output of the sensor records will be made available to authorized users through a designated website.

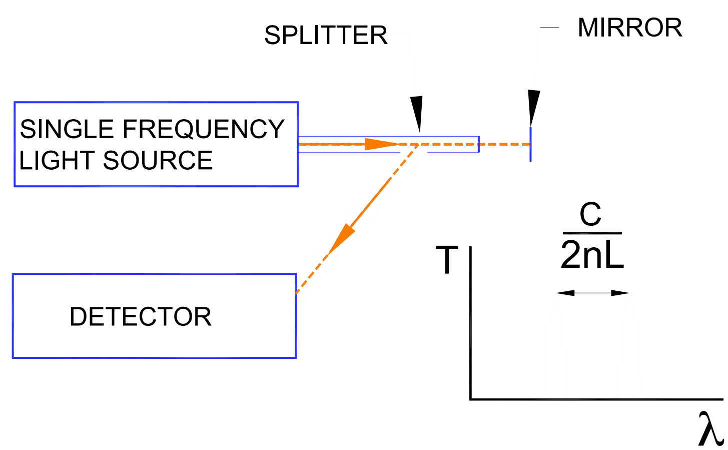


**Figure 7 Fabry-Perot strain sensor schematic**

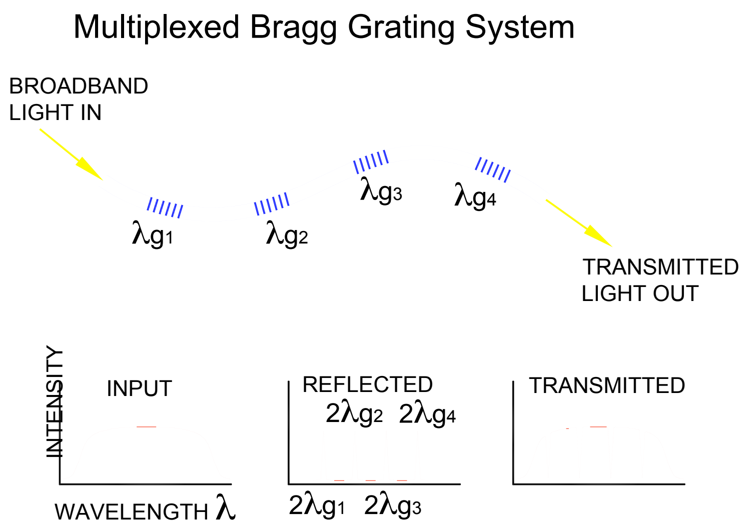


**Figure 8 Bragg Grating strain sensor schematic**

### 3.5.2 Related Work

Research related to the work proposed herein is currently being carried out under other projects by the principal investigators at the University of Hawaii at Manoa. This work is described in this section.

#### 3.5.2.1 Sensor evaluation

To identify the most suitable fiber optic sensor for the work proposed herein, a laboratory test program is currently underway at the University of Hawaii structural engineering laboratory. Samples of FRP (both carbon and glass fiber) with embedded fiber optic strain sensors will be fabricated and tested under static and fatigue tension loading in a hydraulic servo-controlled MTS universal test frame in the lab. Sensor accuracy will be compared with externally applied electrical resistance strain gages and electronic extensometers attached to the specimen during testing. The static tests will be used to verify the accuracy of the FOS at small strains and their ability to monitor ultimate conditions as the FRP nears rupture. The fatigue tests will be used to verify the repeatability and long-term stability of FOS strain readings after numerous cycles simulating serviceability conditions for the project bridge.

This evaluation program is being conducted with current funding from the Hawaii Department of Transportation and will evaluate both Fabry-Perot and Bragg Grating sensors. The most suitable sensor will then be selected for the full-scale bridge application.

#### 3.5.2.2 Previous FRP retrofit of prestressed T-beams

The application of FRP as shear reinforcement to the webs of prestressed T-beams is currently under investigation in the structural engineering laboratory at the University of Hawaii under another Hawaii DOT funded program. This program was principally concerned with the performance of field installed Carbon FRP pre-cured strips as tension reinforcement for a prestressed concrete T-beam in the Ala Moana Shopping Center parking structure. To prevent a premature shear failure of the test beam and control specimen, CFRP fabric was applied to the webs of the beams as shown in Figure 9.

Two shear retrofit schemes were considered. One consisted of closed hoop CFRP stirrups passing through slots cut in the top slab (Figure 10) while the second considered CFRP sheets bonded to each side of the web (Figure 11). In both systems, anchorage of the CFRP at free ends and reentrant corners was provided by means of steel tubes and through bolts as shown in Figure 10 and Figure 11. Tests of the shear spans in the control specimen showed that both types of shear retrofit were effective in substantially increasing the shear strength of the beam.

**Figure 9 Flexural test of control beam with CFRP shear reinforcement**

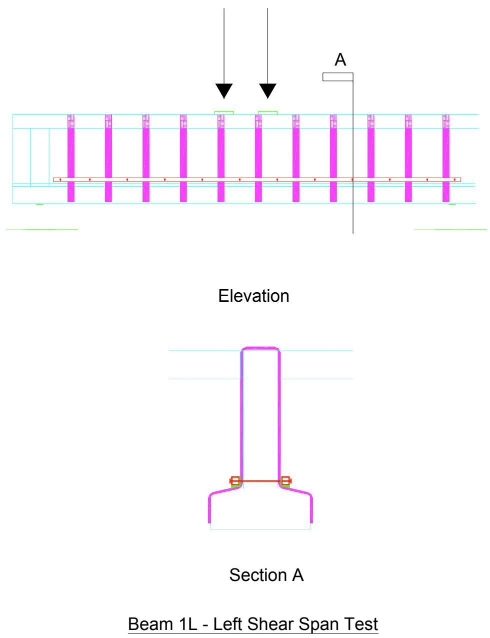


**Figure 10 Test of CFRP stirrup shear retrofit**

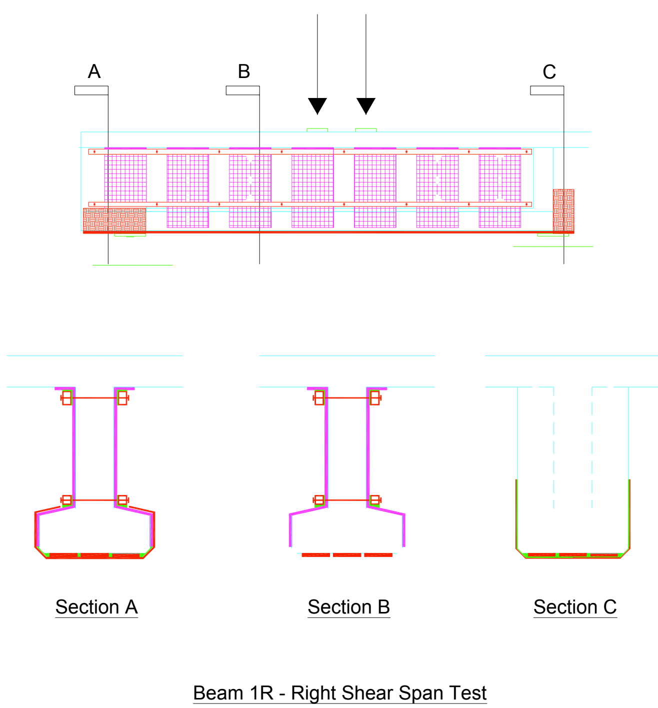


**Figure 11 Test of CFRP sheet shear retrofit**

#### 3.5.2.3 FRP shear retrofit of cracked prestressed T-beams

A third T-beam, nominally identical to the control specimen, will be used to evaluate the performance of CFRP shear retrofit applied over existing shear cracks. This beam already has some web shear cracks (Figure 12). Preloading will be used to induce additional shear cracks before application of the CFRP shear retrofit. Fiber optic sensors selected in the laboratory investigation described above will be embedded in the CFRP shear reinforcement at the crack locations and at pre-defined distances from the crack.

This beam will be tested in shear to monitor the performance of the CFRP and to evaluate the FOS output. The beam will be subjected to a number of loading cycles simulating serviceability conditions before being tested monotonically to failure. The FOS system will be evaluated based on its ability to detect the onset and extent of FRP delamination.

This work is part of the same HDOT-funded project under which the sensors are being tested (section 3.5.2.1).

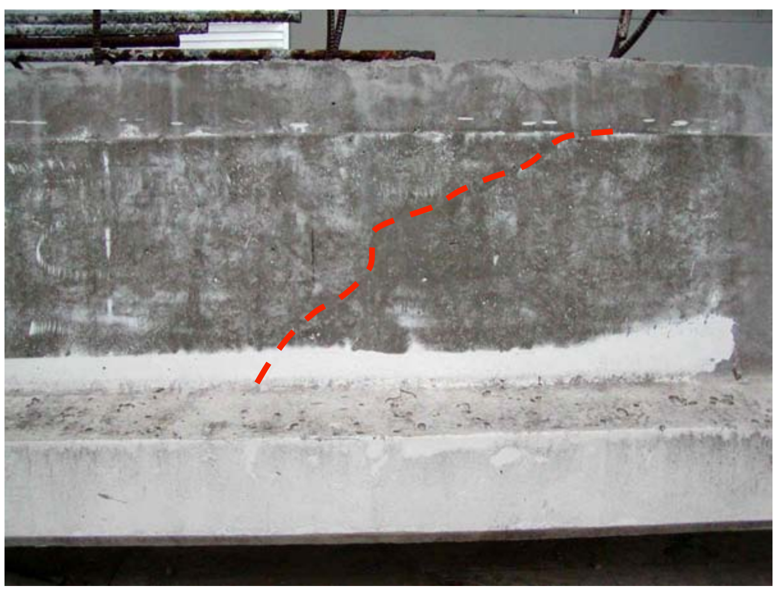

**Figure 12 Hairline shear crack (in red) in prestressed concrete beam**

### 3.5.3 Application to the Salt Lake Boulevard Bridge

In the proposed program, the FOS system for monitoring strain in FRP laminates will be deployed on the Salt Lake Boulevard Bridge during application of the shear retrofit. Installation of the fiber optic strain gages will be performed by UH personnel, in conjunction with the FRP applicator so as not to delay the construction project or to jeopardize the quality and performance of the FRP laminates. Approximately 30 fiber optic strain gages and associated thermocouples will be installed in the FRP shear reinforcement. These gages will be monitored on a continuous basis by automated data loggers installed in weatherproof enclosures under the bridge. The data will be relayed real-time to a server at the University of Hawaii for processing and storage.

## 3.6 Monitoring

Initial monitoring of all instruments will verify that they are functioning as intended. Data collected during ambient traffic flow, diurnal thermal changes, and the planned load test described below, will be used to evaluate the sensor performance. Once satisfactory sensor performance is confirmed, the data will be made available to HDOT personnel.

The instrumentation system will be monitored continuously after installation. The data logger will relay the data automatically to a designated computer in the Department of Civil and Environmental Engineering at UH. The data will be processed automatically and made available for viewing by authorized users. A limited access website will be established to present relevant data for review by transportation officials in the City and County of Honolulu and HDOT on an ongoing basis. This system will continue to monitor, process, display and store all data collected over the project period. UH personnel will maintain the instrumentation in good working condition throughout the project.

Bi-annual visual inspections will be made of the FRP installation, strain sensors and data logger to validate the data received from the instrumentation. Any areas of FRP delamination detected by the instrumentation or during field inspections will be brought to the immediate attention of City and County of Honolulu personnel.

## 3.7 Load Test

### 3.7.1 Introduction

To evaluate the performance of the instrumentation system, a load test will be performed on the structure soon after completion of the FRP retrofit. The load test will be designed to induce shear strains in the FRP shear laminates. The strain determined from the FOS sensors will be compared with that predicted by an analytical model of the bridge girder.

### 3.7.2 Deflection Measurements

An overall deflected shape of the bridge spans provides vital insight into the structural performance during the load test. This deflected shape will be compared with the analytical model to verify assumptions about bridge properties made while developing the analytical model.

An optical survey of the roadway surface will be performed prior to placing load on the bridge and will be compared with subsequent surveys under load to produce deflected shapes for each loading condition. Deflection measurements will also be made using LVDT displacement transducers attached to the soffit of the bridge with spring-loaded lines to the stream invert below. Relative movement between the bridge and the ground will then represent deflection of the bridge under load. A taut-wire base-line system may also be used for monitoring the girder deflections if access to the bottom of the stream is problematic. This system is based on a reference line provided by a taut piano wire, and LVDT displacement measurements between this reference and the bridge girders.

A system of GPS sensors will be used to confirm the deflections obtained by the direct measurements. These sensors are currently being evaluated for use on the Kealakaha Bridge on the Island of Hawaii, but will be available for temporary installation at the Salt Lake Blvd. Bridge during load testing. A reference GPS sensor will be located over a known benchmark away from the bridge structure. Two additional GPS sensors will be placed at locations on the bridge where deflection measurements are required. By correcting their location with respect to the known reference sensor, these local sensors will provide accurate three-dimensional location of their position during loading.

### 3.7.3 Load Application

The load to be applied during the load test will be determined based on the analytical model and the design capacity of the bridge. The load will be applied by means of weighted trucks positioned appropriately on the bridge roadway. Approval by the City and County of Honolulu will be obtained prior to any load testing.

### 3.7.4 Evaluation of Results

Once corrected for thermal effects, the measurements taken during the load test will be compared with the analytical predictions obtained from the computer analysis. The strains measured in the FRP shear retrofit will be evaluated for signs of delamination, particularly adjacent to the existing shear cracks. The results of this load test will be retained for possible comparison with a future load test in the event concerns arise over the long-term performance of the FRP retrofit. An interim project report will detail the load test results and findings.

## 3.8 Analytical Work

### 3.8.1 Background

The proposed project aims at evaluating the performance of the FRP-strengthened bridge using fiber optic strain gages. While these sensors provide high-fidelity performance that is particularly useful for the proposed experimental study, they are more costly than traditional strain gages. As a result, it is desirable to optimize the number and placement of gages. Instrumentation should be placed in the most appropriate locations to monitor most efficiently the desired performance variables. Hence, an analytical study, which can provide a useful guide regarding the placement of strain gages, is required. The analytical study also provides benchmark data against which the load test results can be evaluated. Alternatively, the results of the load test will provide a means to calibrate the assumed input parameters such as material properties and support conditions for the analytical model.

### 3.8.2 Proposed Approach

#### 3.8.2.1 Computational model

In the proposed analytical study, a finite-element model will be developed based on existing computational procedures and mechanical theories for the constituent materials of the FRP-strengthened bridge. In what follows, the major strategies to build the computational model are presented.

First, the finite-element model will be formulated considering the three-dimensional (3-D) geometry of the structure. Although two-dimensional (2-D) formulations can be used effectively to predict accurately the behavior of many structural systems, the AASHTO-type girders used for the bridge necessitate the use of a 3-D model. Non-rectangular cross sections of AASHTO girders will result in non-trivial stress distributions, which will be affected further by the presence of the FRP reinforcement over the web and the reentrant corners between the web and flange. Because the effect of FRP shear reinforcement is to be evaluated, the stresses and strains in the web of the girder need to be predicted accurately, and only a 3-D model can capture the behavior associated with this type of geometry.

Mechanical constitutive equations for concrete, reinforcing steel, and FRP laminates should also be selected carefully to obtain accurate and reliable results. It is not necessary for the computational model to predict the ultimate failure mechanism involving debonding of steel reinforcement and delamination of FRP laminates, because the proposed load test will be conducted within the range of service load level. The analytical model will evaluate only the immediate effect of the FRP reinforcement regarding the localized stiffness enhancement and the FRP strains; debonding of the reinforcement and laminates will not be considered. Thus, it will be assumed that perfect bond exists between concrete and steel. The bond between the concrete and FRP laminates will be predetermined (i.e., the debonding process will not be simulated). However, the model should be capable of modeling stiffness degradation associated with existing cracks and permanent deformation from additional loading. Detailed modeling strategies for each material are given below.

*Concrete*

Shear failure in reinforced concrete structures is induced by tensile cracking, leading to degradation of stiffness in the direction normal to the crack. Although classical plasticity theory can be applied effectively to the situations in which concrete is primarily in compression, a version of fracture mechanics is required to model the zones undergoing tensile cracking. In this study, the plastic-damage model (Lubliner et al. 1989) will be used to model the inelastic behavior of concrete. This model provides a framework that combines the plasticity and damage theory enabling the consideration of stiffness degradation and strength reduction as a result of cracking as well as plastic deformation. Rahimi and Hutchinson (2001) applied this model to FRP-strengthened reinforced concrete beams, and reported good correlation between experimental and analytical results.

*Steel*

Steel reinforcement will be incorporated into the finite-element model as 1-D line elements. Although it is expected that steel reinforcement will behave, primarily, elastically under loading conditions at service level, it may undergo plastic deformation in the zones of tensile cracking after the surrounding concrete loses a substantial portion of its initial stiffness. In this study, the classical $J_2$ plasticity with isotropic hardening will be applied to model the elastoplastic behavior of steel reinforcement.

*FRP*

FRP laminates are linearly elastic until fracture, and will be modeled as such. However, they are anisotropic materials. The anisotropy is due to the direction of the embedded fibers, and the properties depend on the orientation of the reference axes (Daniel and Ishai 1994). The anisotropy will be included in the model used herein.

#### 3.8.2.2 Analytical study

The proposed analytical study will consist of the following two steps of numerical experiments employing the finite-element code based on the computational model discussed above.

First, the maximum design load will be applied to the bridge model without FRP reinforcement so that the greatest shear force will develop in the girder. The intent of this preliminary numerical experiment is to introduce in the computational model the shear cracks that are present in the bridge. From the computational point of view, this is tantamount to adjusting the damage variables to the existing levels.

In the second step, the full bridge model with FRP reinforcement will be considered. The load test after retrofit will be simulated, and the results will be used to provide information regarding the critical positions where strain gages should be installed. While input parameters for the model such as modulus of elasticity of concrete can be obtained from a core of the bridge, comparison of the computational and experimental results will enable the calibration of other parameters for the analytical model, such as concrete compressive and tensile strength and support conditions. The results will also provide the benchmark data against which the load test results can be evaluated.

### 3.9 List of References


ACI (2002). 'Guide for the design and construction of externally bonded FRP systems for strengthening concrete structures.' ACI 440R-02, American Concrete Institute, Farmington Hills, MI.

Aidoo, J., Harries, K.A., and Petrou, M.F. (2002). 'Fatigue behavior of CFRP-strengthened reinforced concrete bridge girders.' International Conference on Composites in Infrastructure, ICCI 2002, San Francisco, June.

Daniel, I. M. and Ishai, O. (1994). *Engineering mechanics of composite materials*. Oxford University Press, New York.

Lubliner, J., Oliver, J., Oller, S., and Onate, E. (1989). 'A plastic-damage model for concrete.' *International Journal of Solids and Structures*, 25(3), 299-326.

McKinley, B., Aarnes, K.A., and Boswell, L. (2002). 'Bridge monitoring using an optical fibre sensor system.' Proceedings of the IABSE Symposium Melbourne 2002, Melbourne, Australia

Park, S. H., Robertson, I. N., and Riggs, H. R. (2002). 'A primer for FRP strengthening of structurally deficient bridges.' University of Hawaii at Manoa Research Report UHM/CE/02-03, 76 pp.

Rahimi, H. and Hutchinson, A. (2001). 'Concrete beams strengthened with externally bonded FRP plates.' *Journal of Composites for Construction,* ASCE, 5(1), 44-56.

Shigemura, Lau, Sakanashi, Higuchi & Associates (2001). 'Final report, bridge no. 911, Salt Lake Boulevard Bridge over Halawa Stream.' Inspection and Load Rating of Bridges II for the City and County of Honolulu, Department of Design and Construction, Honolulu, HI.

# 4.0 Literature Review on Bond between FRP and Concrete

## 4.1 Introduction

Fiber reinforced polymer (FRP) has become one of the most popular materials for strengthening and retrofit of existing reinforced concrete (RC) structures in the past decade. Its popularity is explained by its advantageous characteristics as compared to other solutions, including corrosion resistance, high strength to weight ratio, and easy site handling.

The FRP material is generally bonded to the concrete surface using resin or epoxy in situ to form a composite structure consisting of the original RC member and the FRP. The bond between concrete and FRP plays a very important role in the performance of the retrofitted structure. For beams strengthened for flexure, five failure modes have been identified (Teng, 2002) and are referred to as (1) flexural failure by FRP rupture, (2) flexural failure by crushing of compressive concrete, (3) shear failure, (4) plate-end debonding failure, and (5) intermediate crack-induced interfacial debonding failure. Four failure modes have been observed when RC beams are strengthened for shear (Teng, 2002), including (1) shear failure with FRP rupture, (2) shear failure without FRP rupture, (3) shear failure due to FRP debonding and (4) local failures. Of all these failure modes, FRP debonding is the most common. A number of research efforts have been performed on the mechanics of bonding between FRP and concrete, both experimentally and theoretically. This chapter provides a synopsis of this past research.

## 4.2 Experimental Methods

Experimental researchers have generally used one of three different bonding test methods to study the bond behavior between concrete and FRP. These are referred to as direct tensile tests, shear tests and bending tests as shown in Figure 13 (Nakaba, 2001). The direct tensile test evaluates the bond between FRP and concrete when subjected to tensile stresses normal to the contact surface (a). This is not a common loading condition for FRP in service, but this test is routinely used in the field to evaluate the FRP-to-concrete bond. The double-face shear test consists of two concrete prisms connected by FRP bonded to two opposite surfaces of the concrete prisms (b). Tension force is applied by pulling the reinforcing bars embedded in the concrete prisms. The single-face shear test requires that the concrete block be restrained against rotation (c). The bending tests consist of two separated concrete blocks connected together by FRP on one face, or one block with a partial depth saw cut (d). Transverse FRP is usually applied on one side of the specimen to force failure to occur on the other side. For the inserted shear type specimen, the FRP is sandwiched between two concrete blocks, while steel plates are glued to the outer sides of the concrete (e). Tension is applied to the FRP and steel plates.

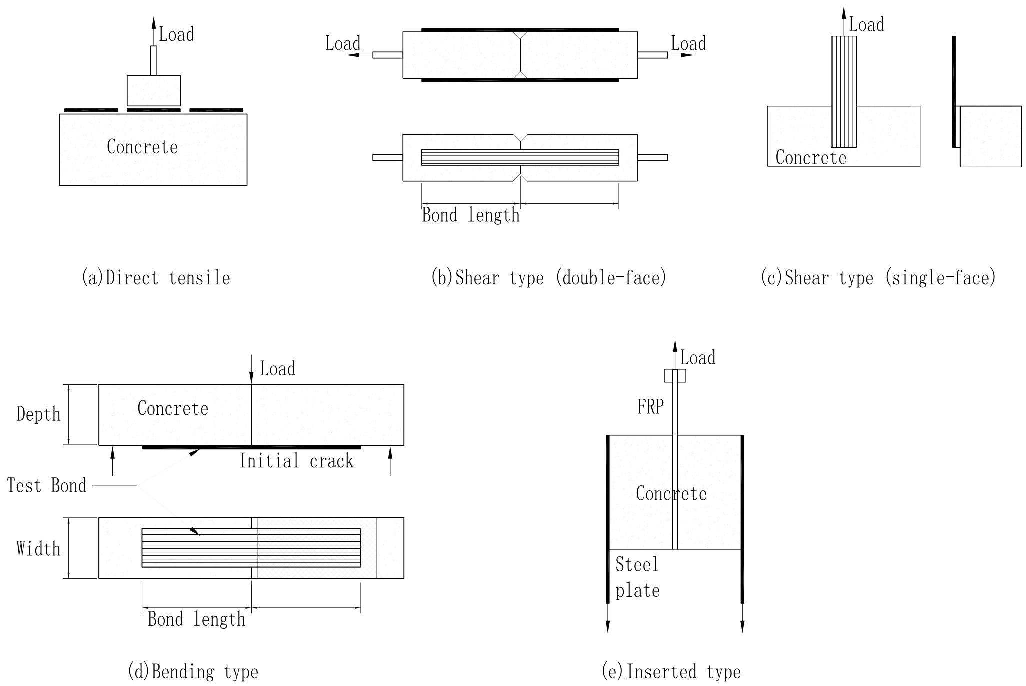


**Figure 13 FRP bond test specimens**

## 4.3 Prior Research Studies

The effects of test method and concrete strength on the bonding behavior of CFRP sheet were studied by Horiguchi and Saeki (1997). Three types of bonding test were conducted with different concrete strengths. High modulus carbon fiber reinforced polymer (CFRP) sheets were used. The target compressive strengths of concrete were 10, 30 and 50 MPa. For the double-face shear test, the concrete specimen was 100 x 100 x 200 mm and the width of CFRP was 75 mm with bonding lengths of 40 mm, 100 mm and 200 mm. For the bending test, the size of concrete block was 150 x 150 x 200 mm. The width of the sheet was 75 mm and the bonding length was 100 mm. For the direct tensile test, the concrete block size was 150 x 150 x 200 mm and the bonding area was 40 x 40 mm. They found the ultimate load increases when the bonding length increases while the average stress decreases. For the three kinds of bonding tests, the direct tensile tests produced the largest average bond stress while the lowest values were obtained from the shear tests. Three types of failure modes were observed; namely, shearing of the concrete, debonding, and FRP rupture. In the shear tests, the CFRP system failed by delamination regardless of the concrete strength. For bending tests and direct tensile tests, failure occurred in the matrix of the concrete when concrete strength was low (10.5 MPa), and by delamination when the concrete strength was 31.4 MPa. When the strength of concrete was 46.1 MPa, the bending test failed by CFRP rupture, while the direct tensile test failed by aggregate/matrix interfacial fracture.

The compressive strength of the concrete played a major role in the bond strength between FRP and concrete. For low compressive strength concrete, the average bonding strength from the three different bonding tests were virtually identical. The higher the concrete compressive strength, the higher the average bonding stress. Empirical equations to estimate the average bond strength were provided as follows:

$$f_b\,(shear) = 0.09\left(f_c^{'}\right)^{\frac{2}{3}} \tag{1}$$

$$f_b\,(bending) = 0.22\left(f_c^{'}\right)^{\frac{2}{3}} \tag{2}$$

$$f_b\,(tensile) = 0.36\left(f_c^{'}\right)^{\frac{2}{3}} \tag{3}$$

where $f_b$ is the average bond strength and $f_c^{'}$ is the concrete compressive strength.

Meada et al. (1997) conducted a total of 37 double-face shear tests. The size of each concrete prism was 100 x 100 mm, while the CFRP width was 50 mm. The surface of concrete was prepared using a sander. Strain gages were placed on the CFRP at a spacing of 10 mm. Three kinds of failure mode were observed: FRP delamination, FRP rupture and concrete fracture. Ultimate loads did not change significantly when the bonding lengths were greater than 100 mm. The maximum load increased with increasing stiffness of the CFRP. The strain distribution has a quadratic form at the early stage of loading but shows bi-linear behavior at the ultimate stage. When the load was relatively small, the load transfer occurred in a small region adjacent to the crack. As FRP debonding occurs, the effective bonding length shifts away from the crack. The mechanics are illustrated in Figure 14. The effective bonding length decreases as the stiffness of the CFRP increases. A non-linear finite element analysis was performed to simulate the strain distribution in the CFRP. Equations to calculate the effective bonding length and ultimate bonding load were developed based on the bi-linear strain relationship as follows:

$$L_e = \exp\left[6.134 - 0.580\ln\left(t \cdot E_{CFRP}\right)\right] \tag{4}$$

$$\tau_{bu} = E_{CFRP} \cdot t \cdot \left(\frac{d\varepsilon}{dx}\right)_0 \tag{5}$$

$$P_{\max} = L_e \cdot b \cdot \tau_{bu} \tag{6}$$

where

$L_e$ = effective bond length (mm)

$t$ = thickness of CFRP (mm)

$E_{CFRP}$ = modulus of elasticity of CFRP (MPa)

$\tau_{bu}$ = average bond strength (MPa)

$\left(\frac{d\varepsilon}{dx}\right)_0$ = strain gradient for effective bond length = $110.2\ \mu / mm$

$b$ = width of CFRP (mm)

$P_{\max}$ = ultimate load on CFRP (N)

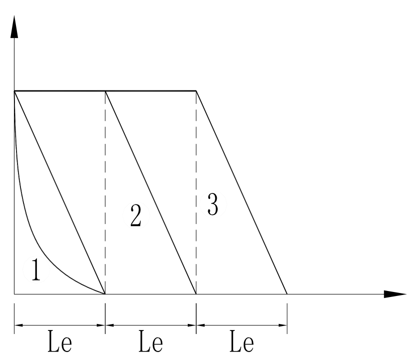


**Figure 14 Schematic strain distribution**

Ueda et al. (1999) carried out an experimental study on bond strength of continuous CFRP sheet. The aspects considered in this study include bond length, width of FRP, stiffness of FRP, loading condition (with/without eccentricity), and method of anchorage (with/without mechanical anchor). Two types of CFRP were used, high strength and high modulus. Five series of shear type tests, designated as A, B, C, D, and E, were conducted.

The surface of the concrete blocks was prepared using a disk sander prior to attaching the CFRP. A total of 28 specimens were tested. In type A and C, tensile load was applied through steel reinforcing bars embedded in the concrete blocks to which the CFRP sheets were attached. Type A was a conventional double-face shear test. Type B were single-face shear tests. For type D and E tests, a hydraulic jack was placed between the concrete blocks to apply a tension force to the CFRP. There were two jacks placed between the concrete blocks in type D. These two jacks were used to apply non-uniform stress in the CFRP. In type E tests, each end of the CFRP strips were anchored by means of steel plates bolted to the concrete base. Based on their tests results, the researchers found that: (1) bond strength does not increase with the increase of bond length for bonding lengths greater than 100mm; (2) the maximum local and average bonding stresses at delamination increase, and the CFRP strain gradient decreases, when the CFRP stiffness increases; (3) the bond strength of CFRP increases with the decrease of CFRP width; (4) non-uniform loading decreases the bond strength and for non-uniform loaded FRP the delamination starts when the maximum strain in FRP reaches the maximum strain for FRP subjected to uniform loading; and (5) steel plate anchors with tensioned bolts enhanced the FRP bond strength.

Brosens and Van Gemert (1999) carried out 24 shear-type bonding tests. The specimen configuration was the inserted shear type as shown in Figure 13 (e). The size of the concrete prism was 150 x 150 x 300 mm. Two widths, 80 mm and 120 mm, and two bonded lengths, 150mm and 200 mm, of CFRP laminate were adopted for these tests. Two specimens were tested for each configuration. The surface of the concrete prisms was sandblasted to remove the weak concrete top layer. The CFRP sheets were Forca Tow Sheets FTS-C1-30 applied to the concrete surface by the wet lay-up method. Based on nonlinear fracture mechanics, a theoretical model to calculate the effective bonding length and the maximum bond strength is provided.

Miller and Nanni (1999) studied the influence of bonded length, concrete strength, and number of plies of CFRP on the bond behavior between FRP and concrete. They selected bending type test specimens to avoid cracking in the bonded length. The carbon fiber sheet used in the test was MBrace CF-130, which is a unidirectional fiber tow sheet. Three kinds of resins (primer, putty and saturant) were used in the application of CFRP to the concrete. The specified concrete strengths were 3000 and 6000 psi. The CFRP strips were applied in single and double plies, with widths of 50.8 mm and 101.6 mm. The concrete surface was sandblasted prior to CFRP application. Three different lengths of CFRP were used. An additional specimen was tested with extra roughening by adding notches on the concrete surface using a hammer and chisel. They report that the bond length had no effect on the bond strength since the bonded lengths were all greater than the effective bond length. The surface preparation had more impact on the bond strength than the compressive strength of the concrete. Increased roughness of the concrete surface improved the average bond strength. The number of CFRP plies increased the average bond strength, but the increase was not proportional to the number of plies. The width of CFRP sheet had no effect on the average bond stress.

Nakaba et al (2001) performed both experimental tests and theoretical analysis of the bonding behavior between FRP and concrete. A double-face shear type test was adopted. The primary test variables were the type of fiber (FRP stiffness), concrete strength, and epoxy putty thickness. The size of concrete prism was 100 x 100 x 600 mm. After reinforcing one side of the concrete prism with FRP laminates the prism was cracked at the center notch using a hammer. The width of the laminates was 50 mm and the bonding length was 300 mm. The fibers used included standard carbon fiber, high-stiffness carbon fiber and aramid. Three specimens were tested with each concrete/epoxy/fiber combination. A total of 36 specimens were tested. LVDTs were used to measure the total displacement and the crack width at the center of the prism. Strain gages were installed on the FRP on one side of the crack at intervals of 15 mm. Most of the specimens failed in debonding while several failed by FRP rupture. The maximum load increased as the stiffness of FRP increased. Epoxy putty thickness had no effect on the maximum load. The increase of concrete strength resulted in an increase in the local bond stress, while the stiffness of FRP had no effect on the local bond stress. A local bond stress - slip model was proposed based on Popovics's equation, as follows:

$$\frac{\tau_b}{\tau_{b,\max}} = \frac{s}{s_{\max}} \cdot \frac{n}{(n-1) + \left(\frac{s}{s_{\max}}\right)^n} \tag{7}$$

$$\tau_{b,\max} = 3.5 \cdot \left(f_c^{'}\right)^{0.19} \tag{8}$$

where

$\tau_b$ = local bond stress, MPa;

$\tau_{b,\max}$ = maximum local bond stress, MPa;

$s$ = slip, mm;

$s_{\max}$ = slip at $\tau_{b,\max}$, $s_{\max} = 0.065mm$; and

$n = 3$ = constant.

The maximum loads and effective bonding lengths were calculated using the proposed model and are in good agreement with their test results.

Harmon et al. (2003) investigated the effect of the resin layer properties between surface-mounted FRP and concrete substrate on bonding strength. They performed an experimental investigation to determine the effect of bond layer properties on the bonding performance using nine bending tests. The concrete block used was 610 mm long x 305 mm high and 305 mm wide, and the FRP strip was 50.8 mm wide. The test parameters were the thickness of bonding layer, the shear modulus of the bonding layer resin system, the thickness and stiffness of the FRP layer, the concrete strength, and the bonding length. They found that the thickness and shear modulus of the bond layer are critical to the bond performance, which contradicts the conclusion from Nakaba et al (2001). They also conclude that the bond stress is proportional to $\sqrt{f_c^{'}}$ . Harmon et al. (2003) also tested five beams reinforced with conventional reinforcement plus CFRP as external flexural reinforcement to verify the design equations developed from the beam bonding tests. The five beams used different fibers and different resin systems. An analytical model was proposed and used to calculate the test beam capacities.

## 4.4 Summary

It is clear from this literature review that there are still many unknown factors involved in the bond performance of FRP materials epoxied to the surface of concrete members. Different researchers have made contradictory conclusions, and various different prediction models have been proposed. Considerable additional research is required to characterize more accurately the bond performance of externally applied FRP systems so as to predict their performance under design conditions.

## 4.5 References

Brosens, K., Gemert, D.V. (1999), "Anchorage Design for Externally Bonded Carbon Fiber Reinforced Polymer Laminates", *Fiber Reinforced Polymer Reinforcement for Reinforced Concrete Structures,* Proceedings of Fourth International Symposium, SP-188, C. W. Dolan, S. H. Rizkalla, A. Nanni, eds., American Concrete Institute, Farmington Hills, Mich., pp. 635-645.

Harmon, T.G., Kim, Y.J., Kardos, J., Johnson, T., Stark, A. (2003), "Bond of Surface-Mounted Fiber-Reinforced Polymer Reinforcement for Concrete Structures", *ACI Structural Journal*, V. 100, No. 5, September-October, pp. 557-564.

Horiguchi, T., Seaki, N. (1997), "Effect of Test Methods and Quality of Concrete on Bond Strength of CFRP Sheet", *Non-Metallic (FRP) Reinforcement for Concrete Structures,* Proceedings of the Third International Symposium, V. 1, pp. 265-270.

Kamiharako, A., Maruyama, K., and Shimomura, T. (1999), "Evaluation System of Shear Capacity of Reinforced Concrete Members Retrofitted with Carbon Fiber Reinforced Polymer Sheets in Consideration of Bond-Peeling Characteristics", *Fiber Reinforced Polymer Reinforcement for Reinforced Concrete Structures,* Proceedings of Fourth International Symposium, SP-188, C. W. Dolan, S. H. Rizkalla, A. Nanni, eds., American Concrete Institute, Farmington Hills, Mich., pp. 973-983.

Lorenzis, L.D., Miller, B., and Nanni, A. (2001), "Bond of Fiber-Reinforced Polymer Laminates to Concrete", *ACI Materials Journal*, V.98, No.3, May-June, pp. 256-264.

Meada, T., Asano, Y., Sato, Y., Ueda, T., and Kakuta, Y (1997), "A Study on Bond Mechanism of Carbon Fiber Sheet", *Non-Metallic (FRP) Reinforcement for Concrete Structures,* Proceedings of the Third International Symposium, V. 1, pp. 279-286.

Miller, B. (1999), "Bond between Carbon Fiber Reinforced Polymer Sheets and Concrete", MSc thesis, University of Missouri, Rolla, Mo..

Nakaba, K., Kanakubo, T., Furuta, T., and Yoshizawa, H. (2001), "Bond Behavior between Fiber-Reinforced Polymer Laminates and Concrete", *ACI Structural Journal*, V. 98, No. 3, May-June, pp. 359-367.

Teng, J.G., Chen, J.F., Smith, S.T., and Lam, L. (2002), *FRP-strengthened RC Structures*, John Wiley & Sons, London, UK.

Ueda, T., Sato, Y., and Asano, Y. (1999), "Experimental study on Bond Strength of Continuous Carbon Fiber Sheet", *Fiber Reinforced Polymer Reinforcement for Reinforced Concrete Structures,* Proceedings of Fourth International Symposium, SP-188, C. W. Dolan, S. H. Rizkalla, A. Nanni, eds., American Concrete Institute, Farmington Hills, Mich., pp. 407-416.

# 5.0 Computational Modeling

Computational simulation of FRP-strengthened reinforced/prestressed concrete structures requires, if their ultimate behavior is to be considered, techniques to model important failure mechanisms in the constituent materials and interfaces between them. This literature review focuses on two of the failure: fracture in concrete and debonding of FRP from concrete substrate.

## 5.1 Fracture in Concrete

### 5.1.1 Overview

Many approaches have been developed to simulate numerically fracture in concrete, and they can be classified into two categories: discrete and continuum approaches. In the finite-element context, the discrete crack approach models the crack directly via an inter-element displacement discontinuity, and the continuous part is modeled through classical continuum mechanics. In general, additional criteria are needed to determine the direction of the crack propagation. In the continuum approaches, however, the continuum format is maintained for the entire domain and no inter-element discontinuity is introduced. To represent cracks, either cracking strain is distributed over a certain material volume (smeared crack approach), or strain or displacement discontinuities are embedded in standard finite elements (embedded discontinuity approaches).

### 5.1.2 Discrete crack approach

The discrete crack approach models a crack by means of a separation between element edges upon violating a certain condition of crack initiation. Originated by Ngo and Scordelis (1967), the discrete crack approach was the earliest method used in concrete fracture simulation, and is suitable for those cases for which the crack path is known in advance, such as in mode I fracture. It can even be used for mixed mode fracture if a reasonable guess of the crack path can be made. For the problem in which the crack path is not known in advance, the discrete approach requires remeshing techniques and a continuous change in nodal connectivity. Although such techniques have been implemented in a few finite element codes, a fully general code is not yet available (Bazant and Planas 1998).

### 5.1.3 Smeared crack approach

An alternative method to model cracking in concrete is the smeared crack approach, in which a cracked solid is dealt with as a continuum. In this approach pioneered by Rashid (1968), the geometric discontinuities induced by cracks are represented by cracking strains distributed over a certain area within the finite element (Rots et al. 1985). Upon crack formation, the local stress-strain relation, which is initially isotropic, is switched to an orthotropic one that reflects the decrease in the stiffness in the direction orthogonal to the crack. The axes of orthotropy are determined based on the conditions at crack initiation.

In accordance with the method dealing with the crack direction, smeared crack approaches can be categorized into fixed, multi-directional, and rotating crack models, in which the orientation of the crack is kept constant, updated in a stepwise manner and updated continuously, respectively (Rots and Blaauwendraad 1989). Despite these distinctions, several assumptions are shared by the three models: the decomposition of the total strain into an elastic part and a part due to cracking; the elastic strain is related to the stress by standard equations of linear elasticity; a crack initializes when the principal stress reaches the uniaxial tensile strength; and a traction-separation law relates the crack opening with the residual stress transferred by the crack (Jirasek and Zimmerman 1998).

Unlike the discrete crack approach, the smeared crack approach has the advantage that the mesh topology is not changed when crack grows. Furthermore, there are no restrictions with respect to the orientation of the crack. Due to these advantages, the smeared crack approach has come into widespread use (Riggs and Powell 1986; Crisfield and Wills 1989) and has been implemented in some commercial finite element codes.

A straightforward use of the traction-separation law, or the strain softening relation, leads, however, to spurious mesh sensitivity in finite-element calculations. In the smeared crack approach, this drawback is resolved by resorting to the crack band model (Bazant and Oh 1983) that smears out the fracture energy over the area in which the crack localizes. It is also observed that numerical solutions obtained by traditional smeared crack models can become erroneous due to the phenomenon called stress locking, i.e., spurious stress transfer across a widely open crack. For the fixed crack model, this is mainly due to the fact that the principal strain axes rotate after the crack initiation while the orientation of the crack is fixed, which causes misalignment between the principal axes of strains and stresses. However, locking is also observed for the rotating crack model. Analysis shows that this phenomenon is caused by a poor kinematic representation of the discontinuous displacement field around a macroscopic crack (Jirasek and Zimmerman 1998). This can be improved by the local enrichment of the kinematic representation of highly localized strains, as is done in embedded discontinuity approaches.

### 5.1.4 Embedded discontinuity approach

In embedded discontinuity approaches, a crack is modeled by inserting, in the interior of a finite element, a discontinuity in strains or displacements. One speaks of a weak discontinuity if the strain undergoes a discontinuity while a discontinuity in the displacement is referred to as a strong discontinuity. The resulting improvement in the kinematic representation of strain localization has been shown to eliminate significantly stress locking. Unlike the smeared crack approach, one can also avoid spurious mesh dependence of the solutions without introducing a crack-band concept that requires element-dependent mesh-regularization parameters. These advantages and the early pioneering works by Ortiz et al. (1987) and Belytschko et al. (1988) have motivated numerous research studies on this approach in recent years (Armero and Garikipati 1996; Dvorkin et al. 1990; Jirasek and Zimmermann 2001a, b; Larsson et al. 1996; Oliver 1996a, b; Wells and Sluys 2000).

As is done in the smeared crack approach, in the embedded discontinuity model, the strain or displacement is decomposed into a continuous and a discontinuous part due to the opening and sliding of a crack. However, the discontinuous part of the deformation is not smeared over a band or an element: rather, it is represented by a discontinuity path that splits the finite element into two separate zones. By introducing the traction-separation law and traction continuity condition (the stresses in the bulk and the tractions across the crack should satisfy internal equilibrium), the discontinuities can be expressed in terms of the nodal displacements.

This embedded discontinuity approach has recently been further developed by Oliver and his co-workers (2004) resulting in a fairly comprehensive concrete fracture analysis procedure that includes an algorithm for tracking multiple cracks.

## 5.2 Debonding of FRP

Debonding of FRP laminates from concrete substrate is an important mode of failure in FRP-strengthened structures because the bond is closely related to the stress transfer between FRP and concrete substrate, thereby critically affecting the performance of the strengthening/rehabilitation by FRP. Debonding can take place in any one of the constituent materials, which include FRP, concrete substrate and adhesive layer, or at the interfaces between the materials, such as between concrete and adhesive or between FRP and adhesive (Buyukozturk et al. 2004).

Debonding failures, like failures of any other materials or structural components, can be investigated by two different approaches: strength and fracture (Buyukozturk et al. 2004). A strength approach involves calculating the bond stresses between the FRP and concrete based on elastic material properties. The calculated stresses are then compared with the ultimate bond strength to predict the load level of debonding failure. This approach was taken by, among others, Aprile et al. (2001), Pesic and Pilakoutas (2003), and Wong and Vecchio (2003).

A fracture approach, on the other hand, recognizes debonding as crack propagation, that is, a progressive failure caused by fracture processes. In fact, past experimental studies indicate that the fracture process associated with debonding can be modeled as strain-softening cohesive fracture in concrete (Ali-Ahmad et al. 2004). Computational studies on debonding failure based on such fracture models started to emerge recently, leading to cohesive crack models (or fictitious crack models) by Borg et al. (2002) and Wu and Yin (2003). It is expected that future improvements will address more sophisticated debonding fracture models based on experimental verifications.

## 5.3 References

Ali-Ahmad, M., Subramaniam, K., and Ghosn, M. (2004). "Fracture analysis of the debonding between FRP and concrete using digital image correlation." *Fracture Mechanics of Concrete Structures*, V. C. Li, C. K. Y. Leung, K. J. Willam and S. L. Billington, eds., 787-793.

Aprile, A., Spacone, E., and Limkatanyu, S. (2001). "Role of bond in RC beams strengthened with steel and FRP plates." *Journal of Structural Engineering, ASCE*, 127, 1445-1452.

Armero, F., and Garikipati, K. (1996). "An analysis of strong discontinuities in multiplicative finite strain plasticity and their relation with the numerical simulation of strain localization in solids." *International Journal of Solids and Structures*, 33, 2863-2885.

Bazant, Z. P., and Oh, B.-H. (1983). "Crack band theory for fracture of concrete." *Materials and Structures, RILEM*, 16, 155-177.

Bazant, Z. P., and Planas, J. (1998). Fracture and size effect in concrete and other quasibrittle materials. CRC Press LLC, Boca Raton, Florida.

Belytschko, T., Fish, J., and Engelmann, B. E. (1988). "A finite element with embedded localization zones." Computer Methods in Applied Mechanics and Engineering, 70, 59-89.

Borg, R., Nilsson, L., and Simonsson, K. (2002). "Modeling of delamination using a discretized cohesive zone and damage formulation." Composites Science and Technology, 62, 1299-1314.

Buyukozturk, O., Gunes, O., and Karaca, E. (2004). "Progress on understanding debonding problems in reinforced concrete and steel members strengthened using FRP composites." Construction and Building Materials, 18, 9-19.

Crisfield, M. A., and Wills, J. (1989). "Analysis of R/C panels using different concrete models." Journal of Engineering Mechanics, ASCE, 115(3), 578-597.

Dvorkin, E. N., Cuitino, A. M., and Gioia, G. (1990). "Finite elements with displacement embedded localization lines insensitive to mesh size and distortions." International Journal for Numerical Methods in Engineering, 30, 541-564.

Jirasek, M., and Zimmermann, T. (1998). "Analysis of rotating crack model." Journal of Engineering Mechanics, ASCE, 124(8), 842-851.

Jirasek, M., and Zimmermann, T. (2001a). "Embedded crack model: I. Basic formulation." International Journal for Numerical Methods in Engineering, 50, 1269-1290.

Jirasek, M., and Zimmermann, T. (2001b). "Embedded crack model. Part II: Combination with smeared cracks." International Journal for Numerical Methods in Engineering, 50, 1291-1305.

Larsson, R., Runesson, K., and Sture, S. (1996). "Embedded localization band in undrained soil based on regularized strong discontinuity theory and finite element analysis." International Journal of Solids and Structures, 33, 3081-3101.

Ngo, D., and Scordelis, A. C. (1967). "Finite element analysis of reinforced concrete beams." Journal of American Concrete Institute, 64, 152-163.

Oliver, J. (1996a). "Modeling strong discontinuities in solid mechanics via strain softening constitutive equations. Part 1: Fundamentals." International Journal for Numerical Methods in Engineering, 39, 3575-3600.

Oliver, J. (1996b). "Modeling strong discontinuities in solid mechanics via strain softening constitutive equations. Part 2: Numerical simulation." International Journal for Numerical Methods in Engineering, 39, 3601-3623.

Oliver, J., Huespe, A. E., Samaniego, E., and Chaves, E. W. V. (2004). "Continuum approach to the numerical simulation of material failure in concrete." International Journal for Numerical and Analytical Methods in Geomechanics, 28, 609-632.

Ortiz, M., Leroy, Y., and Needleman, A. (1987). "A finite element for localized failure analysis." Computer Methods in Applied Mechanics and Engineering, 61, 189-214.

Pesic, N., and Pilakoutas, K. (2003). "Concrete beams with externally bonded flexural FRP-reinforcement: analytical investigation of debonding failure." Composites. Part B: engineering, 34, 327-338.

Rashid, Y. R. (1968). "Analysis of prestressed concrete pressure vessels." Nuclear Engineering and Design, 7, 334-344.

Riggs, H. R., and Powell, G. H. (1986). "Rough crack model for analysis of concrete." Journal of Engineering Mechanics, ASCE, 112(5), 448-464.

Rots, J. G., Nauta, P., Kusters, G. M. A., and Blaauwendraad, J. (1985). "Smeared crack approach and fracture localization in concrete." HERON, 30(1), 1-48.

Rots, J.G., and Blaauwendraad, J. (1989). "Crack models for concrete: Discrete or smeared? Fixed, multi-directional or rotating?" HERON, 34(1), 1-59.

Wells, G. N., and Sluys, L. J. (2000). "Application of embedded discontinuities for softening solids." Engineering Fracture Mechanics, 65, 263-281.

Wong, R. S. Y., and Vecchio, F. J. (2003). "Towards modeling of reinforced concrete members with externally bonded fiber-reinforced polymer composites." ACI Structural Journal, 100, 47-55.

Wu, Z., and Yin, J. (2003). "Fracturing behaviors of FRP-strengthened concrete structures." Engineering Fracture Mechanics, 70, 1339-1355.